

# Synthesis and Analysis of Hyperbranched Oligofluorenes for Optoelectronic Applications<sup>†</sup>

CLARA OROFINO<sup>1</sup>, ANASTASIA KLIMASH<sup>1</sup>, ALEXANDER L. KANIBOLOTSKY<sup>1,2</sup>  
AND PETER J. SKABARA<sup>1,\*</sup>

<sup>1</sup>WestCHEM, Department of Pure and Applied Chemistry, University of Strathclyde,  
Glasgow, United Kingdom

<sup>2</sup>Institute of Physical-Organic Chemistry and Coal Chemistry, 02160 Kyiv, Ukraine

Received: October 19, 2016. Accepted: December 18, 2016.

Monodisperse oligofluorenes have an advantage over their polymeric counterparts due to the precise values of electronic energy levels, which are determined by their well-defined structure. They can be synthesized with high purity and exhibit complete batch-to-batch reproducibility of their physical properties. The extension of oligofluorene dimensionality by branching their conjugated backbone leads to star-shaped conjugated systems and dendrimers. Truxene and isotruxene units are natural branching points for oligofluorene systems, as they comprise the fluorene structure as a subunit and create star-shaped oligomers with a virtually no-core moiety. Dendrimers and star-shaped oligofluorenes exhibit increased solubility, improved film-forming, thermal, optical and electrochemical properties which make them attractive for optoelectronic applications.

*Keywords:* organic semiconductors, organic light-emitting diodes, oligofluorenes, truxene

## 1. INTRODUCTION

Polyfluorenes are efficient solution-processable blue emitters, that show excellent film-forming properties, high hole mobility, great ther-

---

\*Corresponding author e-mail: peter.skabara@strath.ac.uk

<sup>†</sup>The research leading to these results received funding from the H2020-MSCA-ITN-2015/674990 project “EXCILIGHT”.

mal and electrochemical stability. Furthermore, they are easily synthesized and their properties are tunable through modification of the structure or copolymerization[1]. They have been extensively used as electroluminescent materials in polymeric light emitting diodes (PLEDs)[2], photovoltaics[2], field-effect transistors (FETs)[3] and solid state lasers[4].

Chemical purity is a key issue in the performance of optoelectronic devices because impurities and degradation during synthesis, processing and device operation can lead to quenching of the emission. For example, polyfluorenes suffer from the formation of fluorenone groups in the polymer backbone (the non-alkylated or partially alkylated methylene of the fluorene undergoes the formation of C=O bonds via oxidative degradation)[5]. This defect acts as a charge or energy trap and quenches the emission efficiency, which lead to an undesirable green emission and the loss of the saturated blue luminescence of polyfluorenes[6]. The fluorenone defects can be circumvented either by the rigorous monomer purification before a final polymerization step[7] or by using the modified procedure for the monomer synthesis[5]. However, the final polymer properties can suffer from batch-to-batch reproducibility issues and end-group variations.

On the contrary, monodisperse  $\pi$ -conjugated oligomers can be obtained with superior chemical purity by e.g. column chromatography. They are characterized by a well-defined structure of their relatively short and uniform chain, which determines the precise HOMO/LUMO energy levels of the materials, and their properties are completely reproducible[8,9]. Linear oligofluorenes have been synthesized to study the correlation between the chemical structure and molecular conformation, as well as the electronic, thermal, optical and morphological properties of rod-shaped  $\pi$ -conjugated polyfluorene systems, providing an insight to the photophysics of this class of conjugated polymers[10]. The superior environmental stability of monodisperse oligofluorenes compared to their polymeric counterparts has enabled their use as efficient light emitters in organic light emitting diodes (OLEDs)[11], dye-doped cholesteric liquid crystal lasers (DD CLC)[12] and organic field effect transistors (OFETs)[13].

On the other hand, linear oligofluorene, as well as their polymeric analogues, can suffer from  $\pi$ - $\pi$  stacking intermolecular interactions which lead to the formation of excimers, luminescence quenching and decrease in photoluminescence quantum yield (PLQY). Extending the dimensionality of a conjugated system by the branching of its backbone is a way to avoid such interactions and to improve the emissive properties of oligomers[14,15]. In this review we are going to focus first on linear oligofluorene systems with co-monomers that bring to a molecule little or no increase in its dimensionality, and then switch to hyperbranched monodispersed conjugated systems with well-defined structures.

## 2. DISCUSSION

### 2.1 Linear oligofluorene

A series of functional units have been incorporated into linear oligofluorenes mainly to alter their electronic properties. Bryce's group synthesized dibenzothiohene-S,S-dioxide-fluorene co-oligomers (Figure 1-a) as efficient blue light emitters ( $\Phi_{\text{PL}}(\text{sol}) \approx 0.65 - 0.67$ ;  $\Phi_{\text{PL}}(\text{film}) \approx 0.44 - 0.63$ ) with improved electron affinity and stability towards p- and n- doping compared to their oligofluorene analogues[16]. They also studied the donor-acceptor properties of an oligofluorene donor terminated with a C<sub>60</sub> fullerene acceptor on one or on both sides (C<sub>60</sub>-Fl<sub>n</sub> or C<sub>60</sub>-Fl<sub>n</sub>-C<sub>60</sub>)[17]. Furthermore, they isolated a single C<sub>60</sub>-Fl<sub>2</sub>-C<sub>60</sub> molecule on a gold surface with a Scanning Tunneling Microscope (STM) tip and monitored the conductance of the single molecule and elongated it at the junction[18]. They then reported the use of an oligofluorene molecular wire with a zinc porphyrin as an electron donor and a C<sub>60</sub> fullerene as an acceptor at either side (Figure 1-b). The molecules undergo long-range electron transfer from the donor to the acceptor in the excited state due to the increased conjugation through the oligofluorene wire. Furthermore, the charge transfer mechanism can be controlled by temperature[19].

Findlay *et al.* described linear oligofluorenes attached to a 4,4-di-fluoro-4-borata-3a-azonia-4a-aza-s-indacene (BODIPY) unit either in the *meso*-position (Figure 1-c) or in the *beta*-position, and demonstrated the suitability of the materials as down-converters[20]. Aldred and co-workers described the synthesis and properties of a series of oligofluorenes end-capped with tetraphenylethene (TPE) moieties (Figure 1-d). The materials showed fluorescence quenching in solution but efficient blue fluorescence in the solid state ( $\Phi_{\text{PL}} = 0.68$  in PMMA film for n=5). Furthermore, solutions of the materials in tetrahydrofuran:water mixtures with a high percentage of water showed high emission through aggregation induced emission (AIE)[21]. Feng *et al.* developed a series of linear diphenylamino-end-capped oligofluorenes with a 1,2,4-triazole electron-withdrawing core (Figure 1-e). These donor- $\pi$ -acceptor- $\pi$ -donor materials exhibit strong three-photon absorption properties, while the PhN-OF(n)-NPh analogue shows two-photon upconverted deep blue lasing[22].

Huang *et al.* described the synthesis and characterization of donor-acceptor 4,5-diazafluorene-based oligofluorenes and polyfluorenes with lowered LUMO levels compared to the corresponding carbocyclic analogues[23]. Kaeser and co-workers described a series of fluorene-benzothiadiazole or naphthalene co-oligomers (Figure 1-f) with different hydrophilic and hydrophobic alkyl chains that led to the self-assembly of the oligomers into fluorescent nanoparticles[24]. Jäkle's group described a new iterative procedure for the synthesis of a series of fluoreneborane oligomers (Figure 1-g) with decreased LUMO levels and red-shifted absorption and emission properties for longer analogues[25]. The incorporation of the 4-cyanophenyl acceptor

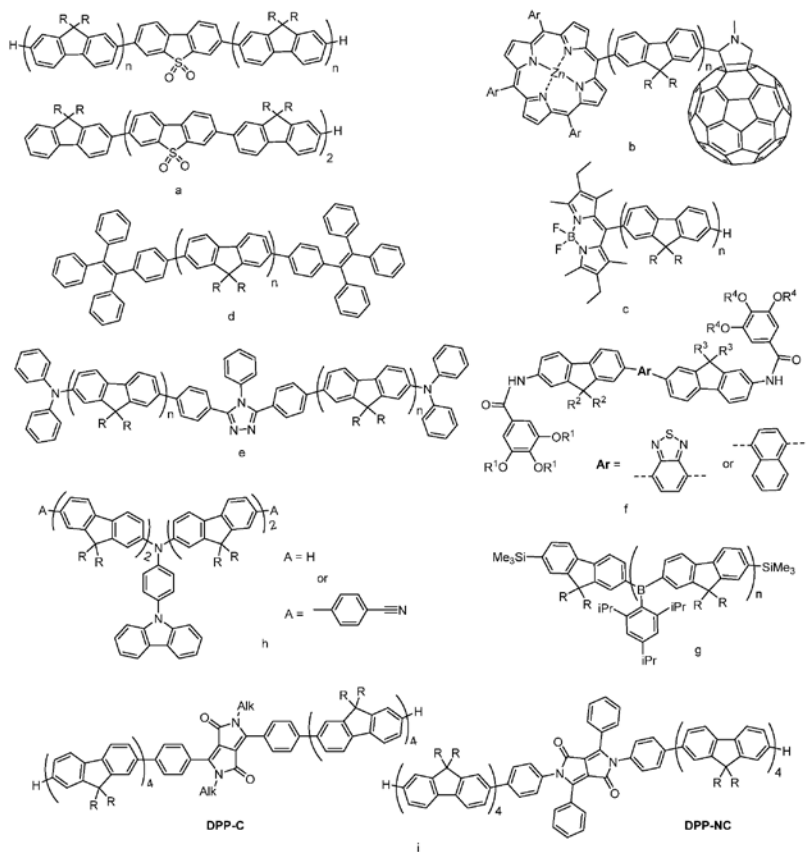


FIGURE 1  
Some linear oligofluorenes reported in the literature.

end-groups, along with a 4-(9H-carbazol-9-yl)aniline donor central unit into the oligofluorene backbone (Figure 1-h,  $A = -C_6H_4CN$ ), yielded blue OLEDs with maximum external quantum efficiencies (EQE) of 4.99 – 7.40 % in the undoped architectures, compared to the EQE of 2.00 % obtained for the analogue without acceptor end-groups (Figure 1-h,  $A = H$ ) and up to 9.40 % in a doped device[26].

The use of oligofluorenes as substituents of 2-phenylpyridine and 1-phenylisoquinoline in Ir(III) complexes was reported by Zhao's group and their photophysical properties at room temperature and at 77 K were compared. The photophysical behavior of these systems was explained by considering an energy transfer process mainly between the triplet ligand-centered (LC) and metal-to-ligand charge-transfer (MLCT) states[27]. Zhou and co-workers described the synthesis of linear oligofluorenevinylenes attached to an anthracene core. Their study suggests that long oligomeric arms can suppress the formation of excimers, which is beneficial for device fabrication[28].

The substitution pattern of a co-monomer unit can heavily affect the physical properties of a material. The DPP-oligofluorene systems **DPP-C** and **DPP-NC** (Figure 1i)[29] have very similar structures with diphenyl-substituted 2,5-dihydropyrrolo[3,4-c]pyrrole-1,4-dione (DPP) as a co-monomer positioned in the middle of an octafluorene conjugated backbone. The only difference is that in the **DPP-C** molecule phenylene linkers are attached to the DPP central unit *via* its 3- and 6- positions, which create a conjugation pathway from the quaterfluorene donors to carbonyl acceptors of DPP and facilitate the intramolecular charge transfer (ICT). On the other hand, **DPP-NC** presents a linear conjugated system with more isolated donor and acceptor units. Not only does this difference affect the electrochemical and optical properties of the materials, it also leads to the appearance of a sharp melting peak in the differential scanning calorimetry (DSC) curve of **DPP-C**, with only a glass transition registered for **DPP-NC**. This was explained by aggregation of **DPP-C** molecules in the solid phase due to electrostatic interactions of quadrupoles created by ICT[29].

Despite this aggregation **DPP-C** showed the narrowing of the spectra in an amplified spontaneous emission (ASE) experiment[29]. The tendency of **DPP-C** to aggregate in the solid state results in the alignment of HOMOs in the aggregates, thus favoring hole mobility and making this compound a promising candidate for OLED applications. The OFET hole mobility of this material was estimated to be  $\sim 1.9 \times 10^{-4} \text{ cm}^2 \text{ V}^{-1} \text{ s}^{-1}$ [30].

## 2.2 From linear oligomers to star-shaped architectures

Star polymers and oligomers consist of three or more linear oligomer arms joined together by a central core. They possess two or three dimensional architecture depending on the nature of the core (flat rigid cores with rigid-rod like arms attached provide a 2D geometry, whereas non-planar cores give rise to 3D structures)[15]. 1D conjugated polymers and oligomers show anisotropic properties due to the conjugation along the linear backbone, but not along the other two dimensions. This issue leads to anisotropic properties in aligned chains of these 1D systems and limitations in their electronic characteristics when they are disordered in the bulk. The increase in dimensionality of star-shaped conjugated systems represents a clear advantage compared to their 1D analogues[31]. The characteristic shape of these materials together with the conjugated nature of the arms provides new electrochemical, optical and morphological properties that make them attractive for optoelectronic applications[32].

The majority of linear oligofluorenes with co-monomers reviewed in the previous section can be considered as systems with a core unit (co-monomer) and one or two oligofluorene arms, depending whether a co-monomer is incorporated at the terminal position or in the middle of the conjugated backbone, respectively. The charge transfer from the arm/arms to a core can lead to the appearance of either dipole or quadrupole moments which, in the case

of neutral systems, can have a significant effect on the supramolecular organization in the solid film. Despite their structural simplicity, some of the aforementioned linear systems present interesting examples of energy transfer. In the case of multidimensional analogues of these linear systems, both charge and energy transfer can be affected by the higher symmetry of the star-shaped molecule, which creates an additional handle to refine the properties of the materials.

A generic relation can be established between the linear oligomers and their star-shaped generations by considering simple symmetry operations over a corresponding monomer unit. If the latter possesses a symmetry point group that includes rotational operations with an order greater than two, the application of such symmetry operations to the whole linear molecule leads to the construction of the corresponding star-shaped system. The application of a  $C_3$  or  $C_6$  symmetry operation to oligo-*p*-phenylene leads to star-shaped systems with 3 or 6 arms, respectively[15]. If only part of the monomer unit has rotational symmetry, the application of the symmetry operation generates a star-shaped system with a new core. In the case of oligofluorenes, the application of  $C_3$  symmetry operations at the centre of the benzene fragment of the monomer leads to star-shaped systems with benzene and truxene cores. Rotational symmetry  $C_n$  (with  $n \geq 3$ ) of the molecule affects the electronic properties such as the degeneracy of HOMO and LUMO levels[15].

Cores with the point group  $D_{2h}$  and four arms can provide diagonal conjugation along the arms through the core, offering an additional means of tuning the band gap of the materials and enhancing the dimensionality of donor-acceptor interactions[33].

### 2.3 Hyperbranched compounds with a truxene core

10,15-Dihydro-5H-diindeno[1,2-*a*:1',2'-*c*]fluorene (truxene) is a polycyclic aromatic system with  $C_3$  symmetry that can be perceived as three overlapping fluorene fragments[34] (see Figure 2). The truxene unit can easily be functionalised at C-2, C-7 and C-12 positions and at the C-5, C-10 and C-15 positions. The C-5, C-10 and C-15 positions are usually derivatized with alkyl

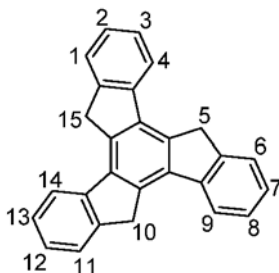


FIGURE 2  
The truxene core with labeling.

chains to increase the solubility and processability of the truxene unit and to reduce intermolecular  $\pi$ - $\pi$  stacking[15].

Truxene has been employed as a starting material for the construction of bowl-shaped fragments of fullerenes[35] and liquid crystalline compounds[36]. *syn*-Trialkylated truxenes have shown self-assembly properties in solution through arene-arene interactions[37] and a 3D core based on truxene was employed as a scaffold for the generation of self-assembled organogels[38].

The core has also been employed to synthesize star-shaped oligomers and dendritic truxene derivatives with  $\pi$ -conjugation to the aromatic core[32,39]. Truxene-based donor acceptor systems for use as multifunctional fluorescent probes have also been described[40]. It has been utilised as a platform for phosphorescent Ru(II) and Os(II) complexes[41]. Truxene has featured in multichromophoric systems with difluoroborondipyrromethene (BODIPY) species as a photoactive core of light harvesting antennae for application in solar energy conversion devices. In these molecules, both the truxene and the BODIPY harvest light but all of it is transferred to the BODIPY through energy transfer processes[42]. The truxene unit has been used as a core in hybrid organic-inorganic multichromophoric star-shaped systems, with their two arms containing Os(II) complexes, and the third arm incorporating different BODIPY moieties[43]. The absorption range of these 2D oligomers extended to the whole UV-vis spectrum, with the BODIPY and Os(II) polypyridyl units acting as a final collectors of the absorbed energy. Truxenes have also been employed in dye sensitised solar cells as a co-adsorbent[44] and as an organic sensitizer[45]. In an interesting report from Scherf *et al.*, truxene has featured in a hyperbranched polytruxene end-capped with donor dyes for optical applications[46]. Sánchez and co-workers described the use of truxene connected to [60]fullerene (C<sub>60</sub>) as electron and energy transduction antennae[47]. Lavelée *et al.* have recently developed highly absorbing truxene-based photoinitiators for polymerization.[48] Truxene has featured as antennae in a multiluminescent organometallic polymer to provide slow energy transfer[49]. It was also employed in a star-shaped chromophore with two-photon excited fluorescence properties[50].

An interesting example of a benzene-cored star-shaped structure (Figure 3-a) and truxene-based dendrimer (Figure 3-b) has been revealed by the Pei group[51]. Modest quantum efficiency values of ~0.16% in OLEDs fabricated from these compounds have been observed, with the electroluminescence spectra (EL) red-shifted compared to those of PL[52].

### 2.3.1. Truxene-based oligofluorene systems

The functionalization of the C-2, C-7 and C-12 positions of truxene with oligofluorenes provides an ideal scenario for the synthesis of virtually no-core two-dimensional trigonal star-shaped oligofluorenes (see Figure 4) [32,53,54].

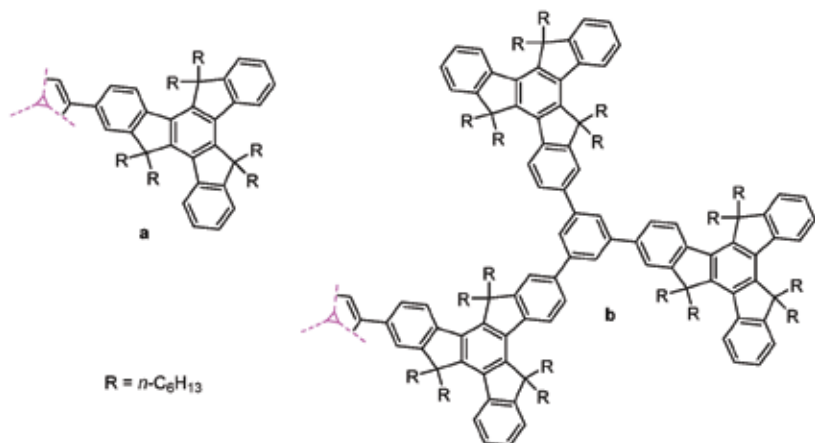


FIGURE 3  
Truxene-related dendritic systems with benzene branching points.

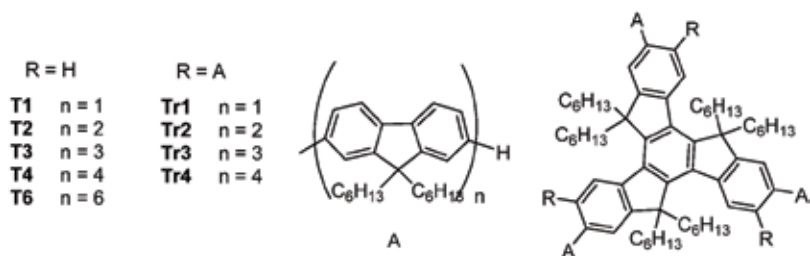


FIGURE 4  
Oligofluorene truxene with the arm length rising from one fluorene unit (**T1**) to four (**T4**) and six (**T6**).

Star-shaped oligofluorene truxenes are very promising materials and have demonstrated excellent properties as the gain medium in organic semiconductor lasers (OSLs)[32,55,56]. Alkyl chains in oligofluorene truxenes act as solubilizing groups as well as spacers preventing intermolecular  $\pi$ - $\pi$  stacking that leads to quenching of light emission. Furthermore, investigating the physical properties of truxene-cored oligofluorenes gives a greater insight into the effective conjugation length of the oligofluorene-truxene family. These nanosized macromolecules show advantages over conjugated polymers because they present monodisperse oligomers with a well-defined and uniform molecular structure that enables the investigation of the impact of molecular structure on electronic, photonic and morphological properties of the materials in the condensed phase.

The absorption spectra of these oligofluorene truxenes in solution and in the solid-state present strong  $\pi$ - $\pi^*$  absorption bands that are red-shifted as the number of oligofluorene units in the arms increases (the maximum absorp-

tion peaks rising from 343 nm for **T1** to 379 nm for **T6**). They are highly fluorescent in solution and in the solid-state with PLQY ( $\Phi_{\text{PL}}$ ) values for the longer oligomers ranging from 0.70 to 0.86 in solution and from 0.43 to 0.60 in the solid state, close to those of polyfluorenes. These molecules are bright blue emitters and their photoluminescence (PL) spectra are red-shifted as the length of the oligofluorene arms increases ( $\lambda_{\text{PL}} \approx 400 - 420$  nm). They all show the typical vibronic structure for polyfluorenes, whose shape is independent of the conjugation length in solution but their relative intensity varies in the solid state[32,57].

Cyclic voltammetry (CV) studies have proved that these materials have good electrochemical stability both to p- and n-doping and have shown that all the oligomers are high band-gap materials (in the range of 3.20 - 3.40 eV)[57]. According to DFT calculations, the degeneracy of the frontier orbitals arising from the symmetry of the molecule is maintained only for truxene itself and the first member of the oligofluorene-truxene series, **T1**[58].

Thermal and morphological stability are key issues for device performance. Thermogravimetric analysis (TGA) of oligofluorene truxene materials shows stability up to 400 °C in an inert atmosphere, increasing slightly as the oligofluorene arm length increases. All the oligomers are amorphous materials at room temperature (although **T1** shows some crystallinity), and present increasing glass transition temperatures from **T1** to **T4**[32].

**T4** ( $\approx 4$  nm molecular radius) has been employed to produce fluorescent microstructures when blended with the UV-photoresist material, 1,4-cyclohexanedimethanol divinyl ether (CHDV), which can be cross-linked by direct laser writing[59]. This encapsulation process enables individual photoprocessing of nanoscopic organic light-emitting molecules, reduces oxygen diffusion and photo-oxidation and makes possible the creation of all-organic optical devices, which had not been achieved so far due to the incompatibility of organic light-emitting molecules with conventional photolithography materials. Furthermore, a fluorescent microstructure of **T4**/CHDV was micropatterned on silicon dioxide using DIP-pen nanolithography.[60] The compound **T3** (3.1 nm molecular radius) has also been blended with CHDV to provide a micro-patterned composite over GaN light-emitting devices (LEDs) as micro pixels, *via* solvent-free inkjet printing. This hybrid GaN/organic device allows the conversion of UV light emitted by the inorganic LED to blue emission (in the visible spectrum) by the oligofluorene truxene material[61]. Additionally, free-standing membranes of **T3**/CHDV blends were prepared, showing ASE thresholds around 80 kW·cm<sup>-2</sup>[62]. The same group described the first use of a monodisperse star-shaped oligofluorene in an encapsulated and mechanically flexible format. The **T3**/CHDV was employed in a DFB laser with an increased stability from a degradation energy dosage of 11.5 J·cm<sup>-2</sup> (in ambient form) to that of 53 J·cm<sup>-2</sup> (for encapsulated material)[63].

Guilhabert and co-workers fabricated and characterized a flexible 4×4 array of organic semiconductor lasers with **T3** as the gain medium. The lasers presented wavelength uniformity across the array with a lasing threshold of 14 kW·cm<sup>-2</sup> and the output could be tuned by 10 nm upon flexing the substrate[64]. Samuel's group developed DFB lasers employing the oligofluorene truxene materials as the gain medium. Their **T3** laser presented a lasing threshold of 515 W·cm<sup>-2</sup> and a very broad wavelength tunability across 51 nm (422 – 473 nm) in the deep-blue region, with lower ASE threshold and higher solid-state PLQY ( $\Phi_{\text{PL}}$  (film) = 0.86), neat gain coefficient and lasing tunability than **T4**[56]. On the other hand, **T4** ( $\Phi_{\text{PL}}$  (film) = 0.73) was employed in a DFB laser with a lower lasing threshold than for **T3** (270 W·cm<sup>-2</sup>). This low threshold was attributed to a low ASE threshold and low waveguide loss coefficient of 2.3 cm<sup>-1</sup> due to the amorphous nature of the **T4** films (the waveguide optical losses of this material within a thin waveguide film are reduced by more than a third in comparison to polyfluorene). Moreover, lasing wavelength tunability has been achieved across 25 nm in the blue part of the spectrum by changing the period of the corrugated substrate of the DFB resonator[55]. Recently, the **T3** star-shaped system was also used as a blue component in a RGB-white laser together with the aforementioned **DPP-C** oligomer as a red lasing material[65].

Radial oligofluorene truxenes with six arms (**Tr1** - **Tr4**) in the C2, C3, C7, C8, C12 and C13 positions of the truxene core (Figure 3) have also exhibited efficient luminescence in the solid state, amorphous characteristics, good solubility in common organic solvents, well-defined molecular size and structure, and high purity *via* column chromatography. They exhibit efficient deep-blue emission with high PLQY ( $\Phi_{\text{PL}}$  = 0.64 – 1.00 in solution and 0.50 – 0.90 in films) and their absorption and emission spectra are blue-shifted with respect to their oligofluorene truxene analogues with three arms (**T1** - **T4**), due to steric hindrance between the core and arms, that leads to a decrease in the degree of conjugation. A DFB laser of **Tr3** afforded a low threshold (109 W·cm<sup>-2</sup>) and wavelength tunability from 421 to 442 nm, achieved by the control of the film thickness (100 - 150 nm)[53].

When the length of oligofluorene arms increases from 3 to 6, molecules exhibit increasing two-photon absorption due to the elongated  $\pi$ -conjugation. The oligomer **T6** shows the threshold for two-photon absorption pumped amplified spontaneous emission of 2.43 mJ cm<sup>-2</sup>, which is the best result for organic semiconductors[54]. It makes these radial oligofluorene truxenes the most suitable candidates for non-linearly pumped light-emitting materials.

### 2.3.2. Oligofluorene-truxene star-shaped systems containing the 2,1,3-benzothiadiazole unit

The electron-deficient character of the 2,1,3-benzothiadiazole (BT) heterocycle can be used for stabilization and spatial localization of the LUMO in

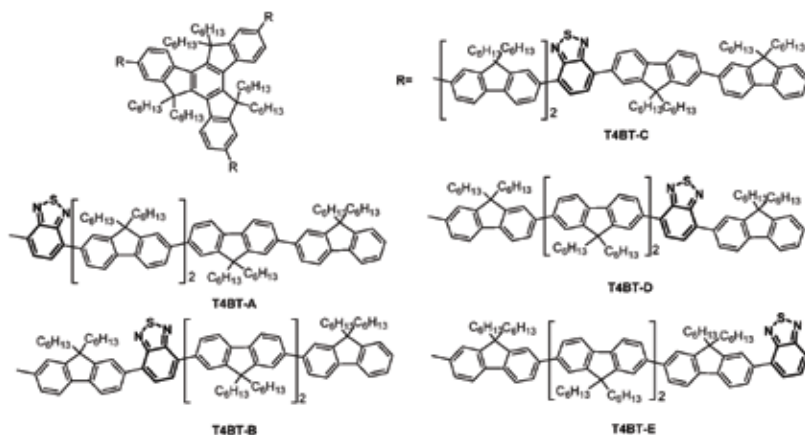


FIGURE 5

Structures of oligofluorene-truxene star-shaped systems containing the 2,1,3-benzothiadiazole unit

conjugated structures and it is widely applied in the design of organic semiconductors. Following the study of the aforementioned oligofluorene truxene structures (**T1-T4**), new **T4**-based compounds with the fused bicyclic 2,1,3-benzothiadiazole molecule inserted sequentially at each of five possible positions were reported (Figure 5)[66].

Absorption spectra in the solid state for compounds **T4BT-A**, **-B**, **-C**, **-D** and **-E** show high energy localized-localized  $\pi$ - $\pi^*$  transition peaks around 220 nm. The delocalized-delocalized  $\pi$ - $\pi^*$  transition for **T4BT-A** and **T4BT-D** show the most intense peak at 362 nm and 370 nm, respectively, with a well-defined shoulder at 320 nm, so transitions between the HOMO and higher lying delocalized unoccupied orbital are split into two components. In the meantime, similar transitions for **T4BT-B** and **T4BT-C** show peaks around 356 nm, with an unresolved shoulder around 320 nm. The characteristics of the spectra correlate with the position of the BT unit in the chain between the outlying conjugated 9,9-dihexylfluorene units and 9,9-dihexylfluorene units attached to the core. The most red-shifted delocalized-delocalized  $\pi$ - $\pi^*$  transition peak is found to be for **T4BT-E**, where the sequence of five 9,9-dihexylfluorene units is involved in transitions. All the members of the **T4-BT** series except **T4BT-E** exhibit a transition from the HOMO delocalized across the oligofluorene arms to the LUMO localized on the BT units with the fitted peak positioned at 445 nm for **T4BT-A** and **T4BT-D** pair and 440 nm for **T4BT-B** and **T4BT-C**. This transition possesses a degree of ICT character and is not present in the spectrum of **T4BTE**. TD-DFT calculations for the latter compound reveal the low oscillator strength for the ICT transition due to a small overlap between the HOMO and LUMO of **T4BT-E**. Photoluminescence spectra show the same kind of correlation with **T4BT-B**

and **T4BT-C** having the most red-shifted PL of 562 nm, **T4BT-A** and **T4BT-D** being slightly blue-shifted (553 nm) and **T4BT-E** having strongly blue-shifted PL at 507 nm.

All the compounds of the series are green light emitters with good thermal stability, solubility and film-forming properties. Efficient electrogenerated chemiluminescence (ECL) has been observed for the **T4BT-B** molecule making this family of compounds promising materials for highly sensitive ECL sensors[67,68].

### 2.3.3 *Truxene-based star-shaped molecules with other fluorene-related and non-oligofluorene arms*

Truxene has been employed as a core for other star-shaped materials with other oligomeric arms. Zhou *et al.* developed a family of star-shaped oligo(fluorene vinylenes) with a truxene core showing two-photon absorption properties, Figure 6-a[69]. Pei's group has investigated extensively the properties of truxenes coupled to different types of oligomeric arms. They developed a series of oligo(*p*-phenylene) functionalized truxenes (Figure 6-b) with 1-4 phenylene units per arm as efficient blue emitters with high glass transition temperatures, good solubility in common organic solvents and good film-forming properties[70]. They also synthesized the oligo(fluorene ethynylene truxenes) (Figure 6-c), that possessed efficient greenish-blue light emission for OLED applications[71]. Similarly, Chen and co-workers described a series of star-shaped oligofluorenes ( $n = 1 - 3$ ) with a tri(ethynyl) truxene core. The materials show a small bathochromic shift in the absorption spectra (both in solution and solid state) and solution PL spectra with respect to their **T1** - **T4** analogues, but a large red shift in the solid-state PL spectra, possibly due to some extent of ordering in the condensed phase[72]. In both types of star-shaped systems an unexpected blue shift and a change in the shape of the solid-state PL spectra occurs when the length of the arms is increased to  $n \geq 3$ . This effect might be a consequence of greater disorder in the condensed state due to the flexible ethynylene linkers between the core and the arms[15].

A series of star-shaped truxenes derivatized with oligothiophenes (Figure 6-d) were also synthesized[39] and applied in OFETs by Pei and co-workers[73]. The same group also investigated the potential use of star-shaped truxene cored materials for organic photovoltaics. Their materials with a truxene core and 3,4-ethylenedioxythiophene (EDOT) units in the arms with  $C_{60}$  end groups (Figure 6-e) have given rise to donor-acceptor systems[74]. They developed dendritic star-shaped systems with the truxene core as a branching point and thienyleneethynylene arms as linkers[74]. They then designed more complex asymmetric truxene-cored materials substituted with thiophen-2-yl and 5-(2-(thiophen-2-yl)vinyl)thiophene-2-yl arms end-capped with 4-(diphenylamino)styryl donor or 2-(4-cyano-5-(dicyanomethylene)-2,2-dimethyl-2,5-dihydrofuran-3-yl)vinyl acceptor

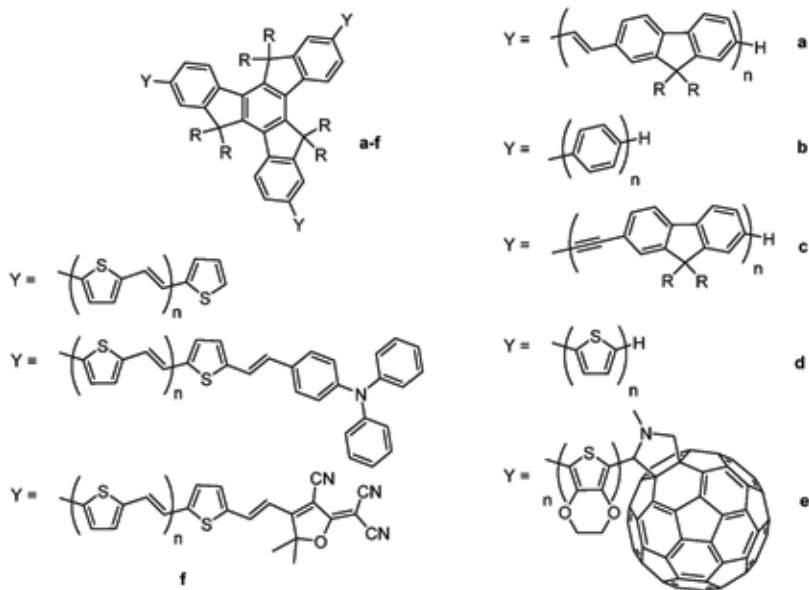


FIGURE 6

Some star-shaped truxene-core materials with oligomeric arms reported in the literature.

groups with potential applications in OPVs (Figure 6-f)[75]. A shape-persistent truxene-core molecule with thiophene-functionalized bisterpyridine Ru(II) complex was also developed by this group for light harvesting applications[76].

#### 2.4. Star-shaped oligofluorene systems with a non-truxene core

Star-shaped oligofluorene architectures with other cores have also been synthesized. Starburst oligofluorene benzene materials (Figure 7-a) are deep-blue emitters and have high PLQYs both in solution and solid state ( $\phi_{PL} = 0.41 - 0.85$  in solution and  $0.21 - 0.56$  in films)[77]. They present good thermal stability and form amorphous films. Their PL spectra present a bathochromic shift with an increase in conjugation length along the arms. CV experiments show good stability towards oxidation and reduction giving evidence of independent processes in the arms, which are not cross-conjugated through *meta*-connections in the core. Tsiminis and co-workers reported the use of a family of starburst materials with a benzene core and three oligofluorene arms (**B1** – **B4**) as the gain media in blue-emitting DFB lasers with low lasing thresholds ( $1.1 \text{ kW}\cdot\text{cm}^{-2}$ ) and high efficiencies (6.6 %). Furthermore, combinations of the **B2-B4** materials in the gain medium enable up to 60 nm spectral tunability[78]. A series of highly twisted materials with a benzene core and six oligofluorene arms has recently been reported. An OLED fabricated with these electroactive materials has shown an external quantum efficiency of 6.8

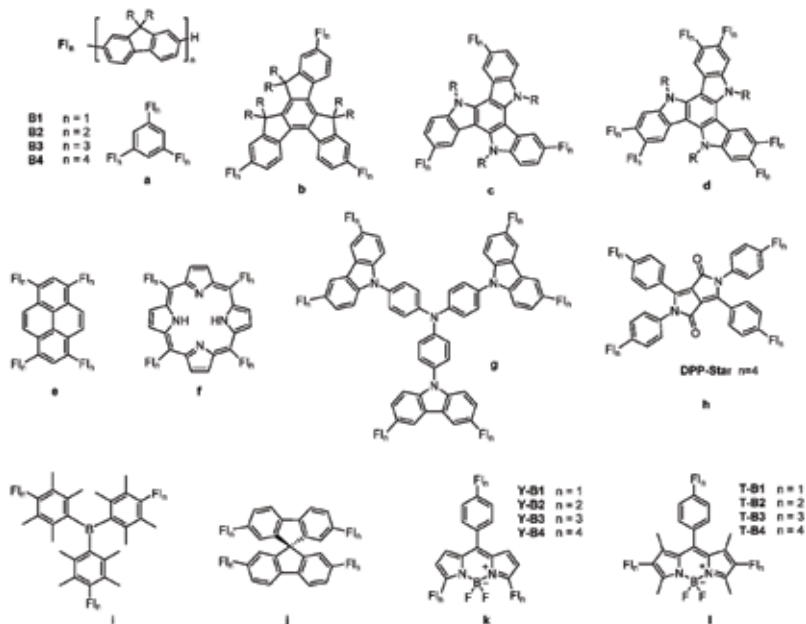


FIGURE 7

Some cores for star-shaped architectures reported in the literature: a) benzene, b) isotruixene, c,d) triazatruxene, e) pyrene, f) porphyrin, g) TCTA, h) DPP, i) tridurylborane, j) spirofluorene, k,l) BODIPY

%, the highest efficiency reported so far for non-doped star-shaped deep-blue electroactive materials[79].

Yang *et al.* synthesised star-shaped oligofluorenes with an isotruixene core (see Figure 7-b). Isotruixene is an isomer of truxene that simultaneously possesses the *para*-, *meta*-, and *ortho*-substituted patterns for the phenylene rings[80]. The presence of the *para*- and *ortho*-linkages between arms of isotruixene – oligofluorene systems leads to stronger electronic couplings between the phenylene rings than in the truxene derivatives, in which only *meta*-linkages are present. This effect is reflected in broader and red-shifted absorption spectra compared to that of truxene analogues. Star-shaped oligofluorene isotruixene derivatives present excellent thermal and electrochemical stability, with blue light emission and high PLQYs ( $\Phi_{\text{PL}} = 0.77 - 0.79$ ). They show higher glass transition temperatures and lower oxidation potentials for generating the hole carrier than their truxene analogues. Furthermore, they have little chain length dependence for the oxidation and reduction potentials and PL spectra (saturation in conjugation with  $n = 2 - 3$ ). This effect arises from the fact that the isotruixene core provides the conjugated pathway between the arms. This contrasts with oligofluorene truxene systems, in which interactions through *meta*-conjugation are negligible and the proper-

ties of the whole molecule are more similar to a single oligofluorene arm[81]. It is interesting to note that, although in the case of the star shaped systems **B1-4** and **T1-4** with *meta*-linked arms there is no conjugation through the core in the ground state, electronic communications between the arms are still possible in the excited state, which leads to redistribution of excitation between the arms[82,83]. More recently, a series of ladder-type oligophenylenes with an isotruxene core with full two-dimensional conjugation both in the ground and excited states has been described[84,85]. These blue emitters present high PLQYs ( $\Phi_{\text{PL}} = 0.73 - 0.82$ ) in  $\text{CH}_2\text{Cl}_2$  solutions[85] and a bathochromic shift with respect to linear analogues, indicating good delocalization of the excitons along the 2D conjugated backbone, owing to the *para/ortho* branching provided by the isotruxene core.

Tri- and hexa-(oligofluorene)triazatruxenes (Figure 7-c,d) have also been synthesised, showing bright blue emission, high quantum efficiencies (up to 0.87 in solution and 0.76 in the solid state) and enhanced hole transport properties compared to those in the oligofluorene truxene series, due to the higher HOMO level of the star-shaped oligofluorenes with a triazatruxene core. These systems have been employed in OLEDs, achieving deep blue electroluminescence with high efficiency and brightness. Their properties as promising gain materials have also been investigated[86,87].

The same group investigated a series of star-shaped cruciform oligofluorenes with a pyrene core (Figure 7-e) as light blue emitters for OLEDs[88]. The materials were also employed as the gain medium in DFB lasers obtaining low lasing threshold (even when increasing the temperature up to 50 °C above their glass transition temperature) and wide wavelength tunability[89].

Recently, a series of star-shaped oligofluorenes with a tetra(phenyl)ethene (TPE) core has been designed to explore aggregation induced emission (Figure 8). The piezofluorochromic properties of the first member of the series

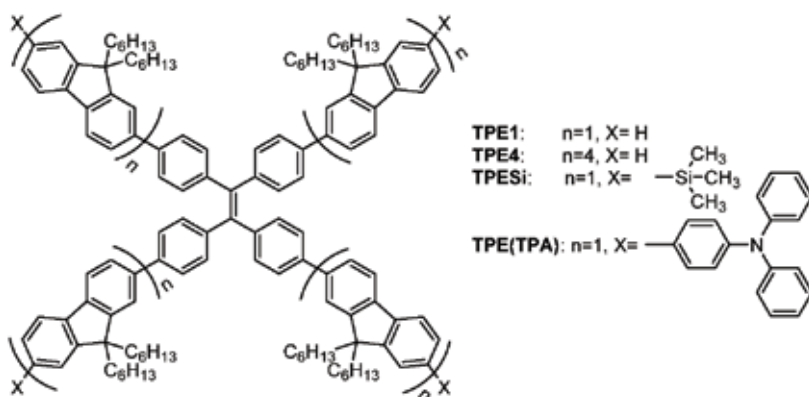


FIGURE 8  
The TPE-core oligofluorene series.

(**TPE1**) are reported and show the potential application of this type of materials in lasing-based sensors[90].

Star-shaped oligofluorenes with a porphyrin core (Figure 7-f) and four arms present blue absorption and red emission due to an energy transfer process, which is enhanced with the increase in the chain length of the arms[91]. The same group also synthesized analogous porphyrin-cored oligocarbazole star shaped materials of up to 7.4 nm radius as efficient red emitters for optical applications[92].

Monodisperse starburst systems with tris(carbazol-9-yl)-triphenylamine (TCTA, Figure 7-g) and six oligofluorene arms of length  $n = 2 - 4$  show bright fluorescence in solution and solid state, high PLQYs and an increased hole mobility due to the presence of the TCTA core, which reduces the energy difference between the HOMO and the work function of ITO. They have been used for the fabrication of OLEDs using the oligomers as the emissive and hole-transporting materials[93].

The star-shaped system with a DPP core and quaterfluorene arms (**DPP-Star**, Figure 7-h)[29] presents an example where the extended core structure and alternating positions of the partially electron-rich and electron-deficient phenylene linkers results in a special kind of aggregation, different from that described for the linear analogue (DPP-C) at the end of section 2.1. In spite of the negative effect of this aggregation on the emissive properties of the material, it still can be useful for design of supramolecular interactions in the bulk of organic semiconductors.

Recently two star-shaped tridurylboranes (Figure 7-i) with three mono or bifluorene arms were described. The materials have excellent solubility and thermal stability and the compound with monofluorene arms has been employed as a host material in a green phosphorescent OLED[94].

Spiro oligofluorenes, in which the two fluorenes of the core have a relative  $90^\circ$  orientation (Figure 7-j) possess good thermal stability towards crystallinity and excellent amorphous film-forming properties. These systems are blue emitters with similar spectroscopic characteristics in the solution and condensed state, and present  $\Phi_{\text{PL}} \approx 0.50$ [95].

Spirobifluorene derivatives in themselves are used as building blocks for the synthesis of materials for organic optoelectronics. Steric hindrance created by the perpendicular arrangement of two parts of the spiro structure suppresses efficiently molecular interactions between  $\pi$ -systems. Spiro compounds demonstrate better solubility, significantly higher glass transition temperature and more intense fluorescence compared to their linear analogs [96]. Structures based on the dispirofluorene-indenofluorene (DSF-IF) unit (Figure 9-m) were extensively investigated in the group of Poriel and Rault-Berthelot and were applied as emitters in OLEDs. DSF-IF consists of two spirobifluorene units linked via a shared phenyl ring and demonstrates advantages of both indenofluorene and dispirofluorene architectures [97]. Absorption spectra for DSF-IFs present bands around 230, 254, 300, 310 nm and

three additional bands at 330-335, 335-340 and 345-350 nm which are well correlated with those observed for indenofluorene at 319, 328 and 334 nm. The observed bathochromic shift is most likely due to the spiro-linkage between fluorene and indenofluorene moieties: interaction between two orthogonally linked  $\pi$  systems results in spiroconjugation, which is also proved by CV studies [98]. An extended analog of the DSF-IF oligomer with fluorene units spiro-linked to positions 6 and 15 of 6,9,15,18-tetrahydro-s-indaceno[1,2-b:5,6-b']difluorene as a central conjugated unit instead of indenofluorene (Figure 9-n) was studied as well, showing a smaller HOMO-LUMO gap resulting from the increase in conjugation of this system [99]. The properties of DSF-IF based compounds can be easily tuned by changing the position of the fluorene substituent in the structure. Thus the fluorescence behavior of the dispiroterfluorene-indenofluorene (2,1-*a*)-DST-IF isomer, possessing a cofacial terfluorene moiety (Figure 9-o), is significantly different from its less hindered analog (1,2-*b*)-DST-IF (Figure 9-p) due to the influence of intramolecular  $\pi$ - $\pi$  interactions between terfluorene units. The optical behavior of both structures was compared with that of their constituents: DSF-IF isomers studied previously in the same group [100] and terfluorene (3-F). As it could be expected, the absorption spectra demonstrate low energy bands around 354-355 nm corresponding to  $\pi$ - $\pi^*$  transitions involving terfluorene units and high energy bands at 343-347 nm attributed to the  $\pi$ - $\pi^*$  indenofluorene transition. Both DST-IF based compounds have an optical band gap of around 3.15 eV which are more comparable to the data observed for terfluorene derivatives than to that of DSF-IF, hence the HOMO-LUMO gap is controlled by the extended  $\pi$ -conjugated system of terfluorene units. The (2,1-*a*)-DST-IF and (1,2-*b*)-DST-IF materials demonstrate deep blue fluorescence in solution but their fluorescence spectra have some significant differences. For both compounds the emission in solution originates mainly from the terfluorene units, but the contribution from frustrated intramolecular excimers is also important for (2,1-*a*)-DST-IF with its face-to-face organization of terfluorene units. The emission of (2,1-*a*)-DST-IF in the solid state is very different from that in solution and is attributed to intramolecular excimer formation resulting from stacked face-to-face terfluorene units. The (2,1-*a*)-DST-IF was used in a single layer SMOLED and demonstrated stable blue emission[101]. Other analogs of DSF-IF containing xanthene instead of the fluorene unit were reported as well, presenting new opportunities for tuning of electronic properties[102]. It was also proven that the position of substituents on the spirobifluorene core leads to important changes in its behavior and these materials can be used as hosts or emitters in OLEDs depending on the nature of the substituents [103,104].

The syntheses of two families of BODIPY-based systems were reported. Oligofluorene arms ( $n = 1-4$ ) are attached in two ways: at the *meso*-position linked via a phenylene unit and  $\alpha$ -position of the BODIPY core (Figure 7-k), or at the *meso*- and  $\beta$ -positions (Figure 7-l) resulting in the formation of Y- and T-shaped

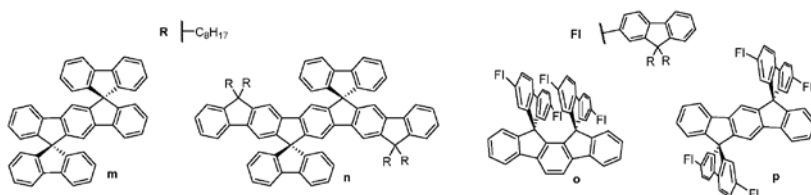


FIGURE 9  
Spirobifluorene-based oligomers.

molecules, respectively[105]. The efficiency of these systems as down-converters for visible light communication was studied recently. Their high illumination performance and short photoluminescence lifetime makes them a promising material for replacing currently used phosphor analogs[106,107]. Recently, by using the blend of **T4BT-B** and **Y-B3**, a fast color conversion has been achieved with a near complete (>90%) energy transfer from the truxene-BT-oligofluorene system to the BODIPY star-shaped oligomer[108].

Other 3D star-shaped oligofluorenes have been described, for example with an adamantane core of tetrahedral architecture[109], 2,4,6-triphenyl-1,3,5-triazine core and *N,N,N',N'*-tetraphenylbenzidine core with flexible spacers[110] or a water soluble material with a polyhedral oligomeric silsesquioxane (POSS) core for cellular imaging[111]. These three-dimensional star-shaped oligofluorene materials have not been studied in as much depth as their two-dimensional counterparts.

### 3. CONCLUSIONS

Hyperbranched oligofluorene systems are proved to be promising materials in the field of organic electronics. The star-shaped architecture improves morphological, electrical and optical characteristics of materials due to the increase in dimensionality. As it could be seen from the examples described above, hyperbranched oligofluorene materials combine the good solubility and excellent film-forming properties of polymers with the precise positions of electronic energy levels of monodisperse systems due to their well-defined structure. A great synthetic versatility in creating star-shaped oligomers can be achieved with complete batch-to-batch reproducibility. Moreover, the star-shaped architecture gives an opportunity for materials scientists to explore intricate electronic communications between the arms of the molecules and the core. The possibility of charge and energy transfer within a star-shaped system and the effect of the symmetry on its electronic properties make this type of conjugated system attractive for developing new materials for one- and two-photon absorption pumped lasers, down-converters, OLEDs, ECL sensors or OPVs.

## ACKNOWLEDGEMENT

The research leading to these results has received funding from the H2020-MSCA-ITN-2015/674990 project “EXCILIGHT”

## REFERENCES

- [1] Grimsdale, A. C.; Chan, K. L.; Martin, R. E.; Jokisz, P. G.; Holmes, A. B. *Chem. Rev.* **109** (2009) 897.
- [2] Beaupre, S.; Boudreault, P.-L. T.; Leclerc, M. *Adv. Mater.* **22** (2010) E6.
- [3] Zaumseil, J.; Donley, C. L.; Kim, J. S.; Friend, R. H.; Sirringhaus, H. *Adv. Mater.* **18** (2006) 2708.
- [4] Heliotis, G.; Xia, R.; Bradley, D. D. C.; Turnbull, G. A.; Samuel, I. D. W.; Andrew, P.; Barnes, W. L. *Appl. Phys. Lett.* **83** (2003) 2118.
- [5] Cho, S. Y.; Grimsdale, A. C.; Jones, D. J.; Watkins, S. E.; Holmes, A. B. *J. Am. Chem. Soc.* **129** (2007) 11910.
- [6] Sims, M.; Bradley, D. D. C.; Ariu, M.; Koeberg, M.; Asimakis, A.; Grell, M.; Lidzey, D. G. *Adv. Funct. Mater.* **14** (2004) 765.
- [7] Craig, M. R.; de Kok, M. M.; Hofstraat, J. W.; Schenning, A.; Meijer, E. W. *J. Mater. Chem.* **13** (2003) 2861.
- [8] Martin, R. E.; Diederich, F. *Angew. Chem. Int. Ed.* **38** (1999) 1350.
- [9] Culligan, S. W.; Geng, Y. H.; Chen, S. H.; Klubek, K.; Vaeth, K. M.; Tang, C. W. *Adv. Mater.* **15** (2003) 1176.
- [10] Geng, Y. H.; Culligan, S. W.; Trajkovska, A.; Wallace, J. U.; Chen, S. H. *Chem. Mater.* **15** (2003) 542.
- [11] Gao, Z. Q.; Li, Z. H.; Xia, P. F.; Wong, M. S.; Cheah, K. W.; Chen, C. H. *Adv. Funct. Mater.* **17** (2007) 3194.
- [12] Chinelatto, L. S., Jr.; del Barrio, J.; Pinol, M.; Oriol, L.; Matranga, M. A.; De Santo, M. P.; Barberi, R. J. *Photochem. Photobiol., A* **210** (2010) 130.
- [13] Yasuda, T.; Fujita, K.; Tsutsui, T.; Geng, Y. H.; Culligan, S. W.; Chen, S. H. *Chem. Mater.* **17** (2005) 264.
- [14] Skabara, P. J.; Arlin, J.-B.; Geerts, Y. H. *Adv. Mater.* **25** (2013) 1948.
- [15] Kanibolotsky, A. L.; Perepichka, I. F.; Skabara, P. J. *Chem. Soc. Rev.* **39** (2010) 2695.
- [16] Perepichka, I.; Perepichka, I. F.; Bryce, M. R.; Palsson, L. O. *Chem. Commun.* (2005) 3397.
- [17] van der Pol, C.; Bryce, M. R.; Wielopolski, M.; Atienza-Castellanos, C.; Guldi, D. M.; Filippone, S.; Martin, N. *J. Org. Chem.* **72** (2007) 6662.
- [18] Leary, E.; Teresa Gonzalez, M.; van der Pol, C.; Bryce, M. R.; Filippone, S.; Martin, N.; Rubio-Bollinger, G.; Agrait, N. *Nano Lett.* **11** (2011) 2236.
- [19] Wielopolski, M.; Rojas, G. d. M.; van der Pol, C.; Brinkhaus, L.; Katsukis, G.; Bryce, M. R.; Clark, T.; Guldi, D. M. *ACS Nano* **4** (2010) 6449.
- [20] Findlay, N. J.; Orofino-Pena, C.; Bruckbauer, J.; Elmasly, S. E. T.; Arumugam, S.; Inigo, A. R.; Kanibolotsky, A. L.; Martin, R. W.; Skabara, P. J. *J. Mater. Chem. C* **1** (2013) 2249.
- [21] Aldred, M. P.; Li, C.; Zhang, G.-F.; Gong, W.-L.; Li, A. D. Q.; Dai, Y.; Ma, D.; Zhu, M.-Q. *J. Mater. Chem.* **22** (2012) 7515.
- [22] Feng, X. J.; Wu, P. L.; Li, K. F.; Wong, M. S.; Cheah, K. W. *Chem. Eur. J.* **17** (2011) 2518.
- [23] Li, W.-J.; Liu, B.; Qian, Y.; Xie, L.-H.; Wang, J.; Li, S.-B.; Huang, W. *Polym. Chem.* **4** (2013) 1796.
- [24] Kaeser, A.; Fischer, I.; Abbel, R.; Besenius, P.; Dasgupta, D.; Gillisen, M. A. J.; Portale, G.; Stevens, A. L.; Herz, L. M.; Schenning, A. P. H. *J. ACS Nano* **7** (2013) 408.
- [25] Chen, P.; Lalancette, R. A.; Jaekle, F. *J. Am. Chem. Soc.* **133** (2011) 8802.
- [26] Zhen, C.-G.; Dai, Y.-F.; Zeng, W.-J.; Ma, Z.; Chen, Z.-K.; Kieffer, J. *Adv. Funct. Mater.* **21** (2011) 699.

- [27] Yan, Q.; Fan, Y.; Zhao, D. *Macromolecules* **45** (2012) 133.
- [28] Zhou, H.; Lu, R.; Zhao, X.; Qiu, X.; Xue, P.; Liu, X.; Zhang, X. *Tetrahedron Lett.* **51** (2010) 5287.
- [29] Kanibolotsky, A. L.; Vilela, F.; Forgie, J. C.; Elmasly, S. E. T.; Skabara, P. J.; Zhang, K.; Tieke, B.; McGurk, J.; Belton, C. R.; Stavrinou, P. N.; Bradley, D. D. C. *Adv. Mater.* **23** (2011) 2093.
- [30] Arumugam, S. B., Roisin E.; Orofino-Pena, Clara; Findlay, Neil J.; Inigo, Anto Regis; Kanibolotsky, Alexander L.; Skabara, Peter J. *Isr. J. Chem.* **54** (2014) 828.
- [31] Roncali, J.; Leriche, P.; Cravino, A. *Adv. Mater.* **19** (2007) 2045.
- [32] Kanibolotsky, A. L.; Berridge, R.; Skabara, P. J.; Perepichka, I. F.; Bradley, D. D. C.; Koeberg, M. *J. Am. Chem. Soc.* **126** (2004) 13695.
- [33] Kanibolotsky, A. L.; Forgie, J. C.; McEntee, G. J.; Talpur, M. M. A.; Skabara, P. J.; Westgate, T. D. J.; McDouall, J. J. W.; Auinger, M.; Coles, S. J.; Hursthouse, M. B. *Chem. Eur. J.* **15** (2009) 11581.
- [34] Gómez-Lor, B.; de Frutos, Ó.; Ceballos, Plácido A.; Granier, T.; Echavarren, Antonio M. *Eur. J. Org. Chem.* **2001** (2001) 2107.
- [35] Gomez-Lor, B.; Gonzalez-Cantalapiedra, E.; Ruiz, M.; de Frutos, S.; Cardenas, D. J.; Santos, A.; Echavarren, A. M. *Chem. Eur. J.* **10** (2004) 2601.
- [36] Li, L.-L.; Hu, P.; Wang, B.-Q.; Yu, W.-H.; Shimizu, Y.; Zhao, K.-Q. *Liq. Cryst.* **37** (2010) 499.
- [37] de Frutos, O.; Granier, T.; Gomez-Lor, B.; Jimenez-Barbero, J.; Monge, A.; Gutierrez-Puebla, E.; Echavarren, A. M. *Chem. Eur. J.* **8** (2002) 2879.
- [38] Tseng, K.-P.; Kao, M.-T.; Tsai, T. W. T.; Hsu, C.-H.; Chan, J. C. C.; Shyue, J.-J.; Sun, S.-S.; Wong, K.-T. *Chem. Commun.* **48** (2012) 3515.
- [39] Pei, J.; Wang, J. L.; Cao, X. Y.; Zhou, X. H.; Zhang, W. B. *J. Am. Chem. Soc.* **125** (2003) 9944.
- [40] Yuan, M. S.; Liu, Z. Q.; Fang, Q. *J. Org. Chem.* **72** (2007) 7915.
- [41] Diring, S.; Ziessel, R.; Barigelletti, F.; Barbieri, A.; Ventura, B. *Chem. Eur. J.* **16** (2010) 9226.
- [42] Diring, S.; Puntoriero, F.; Nastasi, F.; Campagna, S.; Ziessel, R. *J. Am. Chem. Soc.* **131** (2009) 6108.
- [43] Diring, S.; Ventura, B.; Barbieri, A.; Ziessel, R. *Dalton Trans.* **41** (2012) 13090.
- [44] Shi, Y.; Liang, M.; Wang, L.; Han, H.; You, L.; Sun, Z.; Xue, S. *ACS Appl. Mater. Interfaces* **5** (2013) 144.
- [45] Yu, L.; Xi, J.; Chan, H. T.; Su, T.; Antrobus, L. J.; Tong, B.; Dong, Y.; Chan, W. K.; Phillips, D. L. *J. Phys. Chem. C* **117** (2013) 2041.
- [46] Koenen, J.-M.; Jung, S.; Patra, A.; Helfer, A.; Scherf, U. *Adv. Mater.* **24** (2012) 681.
- [47] Sanchez, L.; Martin, N.; Gonzalez-Cantalapiedra, E.; Echavarren, A. M.; Rahman, G. M. A.; Guldi, D. M. *Org. Lett.* **8** (2006) 2451.
- [48] Tehfe, M.-A.; Dumur, F.; Graff, B.; Clement, J.-L.; Gigmès, D.; Morlet-Savary, F.; Fouassier, J.-P.; Lalevee, J. *Macromolecules* **46** (2013) 736.
- [49] Du, B.; Fortin, D.; Harvey, P. D. *J. Inorg. Organomet. Polym. Mater.* **23** (2013) 81.
- [50] Xie, Y. P.; Zhang, X. F.; Xiao, Y.; Zhang, Y. D.; Zhou, F.; Qi, J.; Qu, J. L. *Chem. Commun.* **48** (2012) 4338.
- [51] Cao, X.-Y.; Zhang, W.-B.; Wang, J.-L.; Zhou, X.-H.; Lu, H.; Pei, J. *J. Am. Chem. Soc.* **125** (2003) 12430.
- [52] Cao, X.-Y.; Liu, X.-H.; Zhou, X.-H.; Zhang, Y.; Jiang, Y.; Cao, Y.; Cui, Y.-X.; Pei, J. *J. Org. Chem.* **69** (2004) 6050.
- [53] Lai, W. Y.; Xia, R. D.; He, Q. Y.; Levermore, P. A.; Huang, W.; Bradley, D. D. C. *Adv. Mater.* **21** (2009) 355.
- [54] Guzelturk, B.; Kanibolotsky, A. L.; Orofino-Pena, C.; Laurand, N.; Dawson, M. D.; Skabara, P. J.; Demir, H. V. *J. Mater. Chem. C* **3** (2015) 12018.
- [55] Tsiminis, G.; Wang, Y.; Shaw, P. E.; Kanibolotsky, A. L.; Perepichka, I. F.; Dawson, M. D.; Skabara, P. J.; Turnbull, G. A.; Samuel, I. D. W. *Appl. Phys. Lett.* **94** (2009) 233304.

- [56] Wang, Y.; Tsiminis, G.; Yang, Y.; Ruseckas, A.; Kanibolotsky, A. L.; Perepichka, I. F.; Skabara, P. J.; Turnbull, G. A.; Samuel, I. D. W. *Synth. Met.* **160** (2010) 1397.
- [57] Omer, K. M.; Kanibolotsky, A. L.; Skabara, P. J.; Perepichka, I. F.; Bard, A. J. *J. Phys. Chem. B* **111** (2007) 6612.
- [58] Moreno Oliva, M.; Casado, J.; López Navarrete, J. T.; Berridge, R.; Skabara, P. J.; Kanibolotsky, A. L.; Perepichka, I. F. *J. Phys. Chem. B* **111** (2007) 4026.
- [59] Kuehne, A. J. C.; Elfstrom, D.; Mackintosh, A. R.; Kanibolotsky, A. L.; Guilhabert, B.; Gu, E.; Perepichka, I. F.; Skabara, P. J.; Dawson, M. D.; Pethrick, R. A. *Adv. Mater.* **21** (2009) 781.
- [60] Hernandez-Santana, A.; Mackintosh, A. R.; Guilhabert, B.; Kanibolotsky, A. L.; Dawson, M. D.; Skabara, P. J.; Graham, D. J. *Mater. Chem.* **21** (2011) 14209.
- [61] Wu, M.; Gong, Z.; Kuehne, A. J. C.; Kanibolotsky, A. L.; Chen, Y. J.; Perepichka, I. F.; Mackintosh, A. R.; Gu, E.; Skabara, P. J.; Pethrick, R. A.; Dawson, M. D. *Opt. Express* **17** (2009) 16436.
- [62] Guilhabert, B.; Laurand, N.; Herrnsdorf, J.; Chen, Y.; Mackintosh, A. R.; Kanibolotsky, A. L.; Gu, E.; Skabara, P. J.; Pethrick, R. A.; Dawson, M. D. *J. Opt.* **12** (2010).
- [63] Herrnsdorf, J.; Guilhabert, B.; Chen, Y.; Kanibolotsky, A. L.; Mackintosh, A. R.; Pethrick, R. A.; Skabara, P. J.; Gu, E.; Laurand, N.; Dawson, M. D. *Opt. Express* **18** (2010) 25535.
- [64] Guilhabert, B.; Laurand, N.; Herrnsdorf, J.; Chen, Y.; Kanibolotsky, A. L.; Orofino, C.; Skabara, P. J.; Dawson, M. D. *IEEE Photonics J.* **4** (2012) 684.
- [65] Foucher, C.; Guilhabert, B.; Kanibolotsky, A. L.; Skabara, P. J.; Laurand, N.; Dawson, M. D. *Opt. Express* **24** (2016) 2273.
- [66] Belton, C. R.; Kanibolotsky, A. L.; Kirkpatrick, J.; Orofino, C.; Elmasly, S. E. T.; Stavrinou, P. N.; Skabara, P. J.; Bradley, D. D. C. *Adv. Funct. Mater.* **23** (2013) 2792.
- [67] Dennany, L.; Mohsan, Z.; Kanibolotsky, A. L.; Skabara, P. J. *Faraday Discuss.* **174** (2014) 357.
- [68] Mohsan, Z.; Kanibolotsky, A. L.; Stewart, A. J.; Inigo, A. R.; Dennany, L.; Skabara, P. J. *J. Mater. Chem. C* **3** (2015) 1166.
- [69] Zhou, H.; Zhao, X.; Huang, T.; Lu, R.; Zhang, H.; Qi, X.; Xue, P.; Liu, X.; Zhang, X. *Org. Biomol. Chem.* **9** (2011) 1600.
- [70] Zhang, W. B.; Jin, W. H.; Zhou, X. H.; Pei, J. *Tetrahedron* **63** (2007) 2907.
- [71] Yuan, S. C.; Sun, Q. J.; Lei, T.; Du, B.; Li, Y. F.; Pei, J. *Tetrahedron* **65** (2009) 4165.
- [72] Chen, Q. Q.; Liu, F.; Ma, Z.; Peng, B.; Wei, W.; Huang, W. *Synlett* (2007) 3145.
- [73] Sun, Y. M.; Xiao, K.; Liu, Y. Q.; Wang, J. L.; Pei, J.; Yu, G.; Zhu, D. B. *Adv. Funct. Mater.* **15** (2005) 818.
- [74] Wang, J. L.; Duan, X. F.; Jiang, B.; Gan, L. B.; Pei, J.; He, C.; Li, Y. F. *J. Org. Chem.* **71** (2006) 4400.
- [75] Tang, Z.-M.; Lei, T.; Wang, J.-L.; Ma, Y.; Pei, J. *J. Org. Chem.* **75** (2010) 3644.
- [76] Wang, J.-L.; Chan, Y.-T.; Moorefield, C. N.; Pei, J.; Modarelli, D. A.; Romano, N. C.; Newkome, G. R. *Macromol. Rapid Commun.* **31** (2010) 850.
- [77] Zhou, X. H.; Yan, J. C.; Pei, J. *Org. Lett.* **5** (2003) 3543.
- [78] Tsiminis, G.; Montgomery, N. A.; Kanibolotsky, A. L.; Ruseckas, A.; Perepichka, I. F.; Skabara, P. J.; Turnbull, G. A.; Samuel, I. D. W. *Semicond. Sci. Technol.* **27** (2012).
- [79] Zou, Y.; Zou, J.; Ye, T.; Li, H.; Yang, C.; Wu, H.; Ma, D.; Qin, J.; Cao, Y. *Adv. Funct. Mater.* **23** (2013) 1781.
- [80] Yang, J. S.; Huang, H. H.; Ho, J. H. *J. Phys. Chem. B* **112** (2008) 8871.
- [81] Yang, J. S.; Lee, Y. R.; Yan, J. L.; Lu, M. C. *Org. Lett.* **8** (2006) 5812.
- [82] Montgomery, N. A.; Denis, J.-C.; Schumacher, S.; Ruseckas, A.; Skabara, P. J.; Kanibolotsky, A.; Paterson, M. J.; Galbraith, I.; Turnbull, G. A.; Samuel, I. D. W. *J. Phys. Chem. A* **115** (2011) 2913.
- [83] Montgomery, N. A.; Hedley, G. J.; Ruseckas, A.; Denis, J.-C.; Schumacher, S.; Kanibolotsky, A. L.; Skabara, P. J.; Galbraith, I.; Turnbull, G. A.; Samuel, I. D. W. *PCCP* **14** (2012) 9176.
- [84] Yang, J. S.; Huang, H. H.; Liu, Y. H.; Peng, S. M. *Org. Lett.* **11** (2009) 4942.
- [85] Huang, H.-H.; Prabhakar, C.; Tang, K.-C.; Chou, P.-T.; Huang, G.-J.; Yang, J.-S. *J. Am. Chem. Soc.* **133** (2011) 8028.

- [86] Lai, W. Y.; He, Q. Y.; Zhu, R.; Chen, Q. Q.; Huang, W. *Adv. Funct. Mater.* **18** (2008) 265.
- [87] Levermore, P. A.; Xia, R.; Lai, W.; Wang, X. H.; Huang, W.; Bradley, D. D. C. *J. Phys. D: Appl. Phys.* **40** (2007) 1896.
- [88] Liu, F.; Lai, W. Y.; Tang, C.; Wu, H. B.; Chen, Q. Q.; Peng, B.; Wei, W.; Huang, W.; Cao, Y. *Macromol. Rapid Commun.* **29** (2008) 659.
- [89] Xia, R. D.; Lai, W. Y.; Levermore, P. A.; Huang, W.; Bradley, D. D. C. *Adv. Funct. Mater.* **19** (2009) 2844.
- [90] Orofino, C.; Foucher, C.; Farrell, F.; Findlay, N. J.; Breig, B.; Kanibolotsky, A. L.; Guilhabert, B.; Vilela, F.; Laurand, N.; Dawson, M. D.; Skabara, P. J. *J. Polym. Sci., Part A: Polym. Chem.* **55** (2017) 734–746.
- [91] Li, B. S.; Li, J.; Fu, Y. Q.; Bo, Z. S. *J. Am. Chem. Soc.* **126** (2004) 3430.
- [92] Xu, T.; Lu, R.; Liu, X.; Chen, P.; Qiu, X.; Zhao, Y. *J. Org. Chem.* **73** (2008) 1809.
- [93] Liu, Q. D.; Lu, J. P.; Ding, J. F.; Day, M.; Tao, Y.; Barrios, P.; Stupak, J.; Chan, K.; Li, J. J.; Chi, Y. *Adv. Funct. Mater.* **17** (2007) 1028.
- [94] Zhang, T.; Wang, R.; Wang, L.; Wang, Q.; Li, J. *Dyes Pigment.* **97** (2013) 155.
- [95] Katsis, D.; Geng, Y. H.; Ou, J. J.; Culligan, S. W.; Trajkovska, A.; Chen, S. H.; Rothberg, L. J. *Chem. Mater.* **14** (2002) 1332.
- [96] Saragi, T. P. I.; Spehr, T.; Siebert, A.; Fuhrmann-Lieker, T.; Salbeck, J. *Chem. Rev.* **107** (2007) 1011.
- [97] Horhant, D.; Liang, J.-J.; Virboul, M.; Poriel, C.; Alcaraz, G.; Rault-Berthelot, J. *Org. Lett.* **8** (2006) 257.
- [98] Poriel, C.; Liang, J.-J.; Rault-Berthelot, J.; Barrière, F.; Cocherel, N.; Slawin, A. M. Z.; Horhant, D.; Virboul, M.; Alcaraz, G.; Audebrand, N.; Vignau, L.; Huby, N.; Wantz, G.; Hirsch, L. *Chemistry – A European Journal* **13** (2007) 10055.
- [99] Cocherel, N.; Poriel, C.; Rault-Berthelot, J.; Barrière, F.; Audebrand, N.; Slawin, A. M. Z.; Vignau, L. *Chemistry – A European Journal* **14** (2008) 11328.
- [100] Poriel, C.; Barrière, F.; Thirion, D.; Rault-Berthelot, J. *Chemistry – A European Journal* **15** (2009) 13304.
- [101] Poriel, C.; Rault-Berthelot, J.; Thirion, D.; Barrière, F.; Vignau, L. *Chemistry – A European Journal* **17** (2011) 14031.
- [102] Poriel, C.; Rault-Berthelot, J.; Thirion, D. *The Journal of Organic Chemistry* **78** (2013) 886.
- [103] Thiery, S.; Tondelier, D.; Declairieux, C.; Geffroy, B.; Jeannin, O.; Métivier, R.; Rault-Berthelot, J.; Poriel, C. *The Journal of Physical Chemistry C* **119** (2015) 5790.
- [104] Thiery, S.; Heinrich, B.; Donnio, B.; Poriel, C.; Camerel, F. *The Journal of Physical Chemistry C* **119** (2015) 10564.
- [105] Orofino-Pena, C.; Cortizo-Lacalle, D.; Cameron, J.; Sajjad, M. T.; Manousiadis, P. P.; Findlay, N. J.; Kanibolotsky, A. L.; Amarasinghe, D.; Skabara, P. J.; Tuttle, T.; Turnbull, G. A.; Samuel, I. D. *Beilstein J. Org. Chem.* **10** (2014) 2704.
- [106] Sajjad, M. T.; Manousiadis, P. P.; Orofino, C.; Cortizo-Lacalle, D.; Kanibolotsky, A. L.; Rajbhandari, S.; Amarasinghe, D.; Chun, H.; Faulkner, G.; O'Brien, D. C.; Skabara, P. J.; Turnbull, G. A.; Samuel, I. D. *Advanced Optical Materials* **3** (2015) 536.
- [107] Vithanage, D. A.; Manousiadis, P. P.; Sajjad, M. T.; Rajbhandari, S.; Chun, H.; Orofino, C.; Cortizo-Lacalle, D.; Kanibolotsky, A. L.; Faulkner, G.; Findlay, N. J.; O'Brien, D. C.; Skabara, P. J.; Samuel, I. D. *W. Appl. Phys. Lett.* **109** (2016) 013302.
- [108] Sajjad, M. T.; Manousiadis, P. P.; Orofino, C.; Kanibolotsky, A. L.; Findlay, N. J.; Rajbhandari, S.; Vithanage, D. A.; Chun, H.; Faulkner, G.; O'Brien, D. C.; Skabara, P. J.; Turnbull, G. A.; Samuel, I. D. *W. Appl. Phys. Lett.* **110** (2017) 013302.
- [109] Jeeva, S.; Moratti, S. C. *Synthesis-Stuttgart* (2007) 3323.
- [110] Chen, A. C. A.; Wallace, J. U.; Wei, S. K. H.; Zeng, L. C.; Chen, S. H. *Chem. Mater.* **18** (2006) 204.
- [111] Pu, K.-Y.; Li, K.; Liu, B. *Adv. Mater.* **22** (2010) 643.